

RESEARCH ARTICLE

Resolvin E1 derived from eicosapentaenoic acid prevents hyperinsulinemia and hyperglycemia in a host genetic manner

Anandita Pal¹ | Abrar E. Al-Shaer¹ | William Guesdon² | Maria J. Torres³ | Michael Armstrong⁴ | Kevin Quinn⁴ | Traci Davis¹ | Nichole Reisdorph⁴ | P. Darrell Neuffer³ | Espen E. Spangenburg³ | Ian Carroll¹ | Richard P. Bazinet⁵ | Ganesh V. Halade⁶ | Joan Clària⁷ | Saame Raza Shaikh¹

¹Department of Nutrition, Gillings School of Global Public Health and School of Medicine, The University of North Carolina at Chapel Hill, Chapel Hill, NC, USA

²Department of Biochemistry & Molecular Biology, Brody School of Medicine, East Carolina University, Greenville, NC, USA

³Department of Physiology, East Carolina Diabetes & Obesity Institute, East Carolina University, Greenville, NC, USA

⁴Department of Pharmaceutical Sciences, University of Colorado Denver Anschutz Medical Campus, Aurora, CO, USA

⁵Department of Nutritional Sciences, University of Toronto, Toronto, ON, Canada

⁶Division of Cardiovascular Sciences, Department of Medicine, The University of South Florida, Tampa, FL, USA

⁷Department of Biochemistry and Molecular Genetics, University of Barcelona, Hospital Clínic, Barcelona, Spain

Correspondence

Saame Raza Shaikh, Department of Nutrition, Gillings School of Global Public Health and School of Medicine, 135 Dauer Drive, The University of North Carolina at Chapel Hill, Chapel Hill, NC 27599-7400, USA.

Email: shaikhsa@email.unc.edu

Present address

William Guesdon, School of Immunology and Microbial Sciences, King's College London, Guy's Campus, London, SE1 9RT, UK

Maria J. Torres, Duke Molecular Physiology Institute, Duke University, 300 North Duke Street, Durham, NC 27701, USA

Funding information

This work was supported by NIH R01AT008375 (SRS), NIH P30DK05635 (SRS), NIH R01AR066660 (ES), NIH/

Abstract

Eicosapentaenoic acid (EPA) has garnered attention after the success of the REDUCE-IT trial, which contradicted previous conclusions on EPA for cardiovascular disease risk. Here we first investigated EPA's preventative role on hyperglycemia and hyperinsulinemia. EPA ethyl esters prevented obesity-induced glucose intolerance, hyperinsulinemia, and hyperglycemia in C57BL/6J mice. Supporting NHANES analyses showed that fasting glucose levels of obese adults were inversely related to EPA intake. We next investigated how EPA improved murine hyperinsulinemia and hyperglycemia. EPA overturned the obesity-driven decrement in the concentration of 18-hydroxyeicosapentaenoic acid (18-HEPE) in white adipose tissue and liver. Treatment of obese inbred mice with RvE1, the downstream immunoresolvent metabolite of 18-HEPE, but not 18-HEPE itself, reversed hyperinsulinemia and hyperglycemia through the G-protein coupled receptor ERV1/ChemR23. To translate the findings, we determined if the effects of RvE1 were dependent on host genetics. RvE1's effects on hyperinsulinemia and hyperglycemia were divergent in diversity outbred mice that model human genetic variation. Secondary SNP analyses further

Abbreviations: 12-HEPE, 12-hydroxyeicosapentaenoic acid; 18-HEPE, 18-hydroxyeicosapentaenoic acid; AA, arachidonic acid; DHA, docosahexaenoic acid; DO, diversity outbred; EPA, eicosapentaenoic acid; LA, linoleic acid; NHANES, National Health and Nutrition Examination Survey; PCA, principal component analysis; PUFA, polyunsaturated fatty acid; RvE1, resolvin E1; SPM, specialized pro-resolving mediator.

Anandita Pal and Abrar E. Al-Shaer contributed equally to this work.

This is an open access article under the terms of the Creative Commons Attribution-NonCommercial License, which permits use, distribution and reproduction in any medium, provided the original work is properly cited and is not used for commercial purposes.

© 2020 The Authors. *The FASEB Journal* published by Wiley Periodicals LLC on behalf of Federation of American Societies for Experimental Biology

National Center for Research Resources S10 RR026522-01A1 (NR), NIH R01DK096907 (PDN), Canadian Institutes of Health Research 303157 (RPB), NIH HL132989 (GVH), NIH HL144788 (GVH), SAF15-63674-R (Spanish Ministry of Economy and Science, JC), and 2017SGR1449 (AGAUR Generalitat de Catalunya, JC). This material is also based upon work supported by the National Science Foundation Graduate Research Fellowship Program under Grant No. 1650116 to AEA. Any opinions, findings, and conclusions or recommendations expressed in this material are those of the author(s) and do not necessarily reflect the views of the National Science Foundation

confirmed extensive genetic variation in human RvE1/EPA-metabolizing genes. Collectively, the data suggest EPA prevents hyperinsulinemia and hyperglycemia, in part, through RvE1's activation of ERV1/ChemR23 in a host genetic manner. The studies underscore the need for personalized administration of RvE1 based on genetic/metabolic enzyme profiles.

KEYWORDS

diversity outbred mice, glucose, insulin, polyunsaturated fatty acids, specialized pro-resolving mediators

1 | INTRODUCTION

Circulating levels of eicosapentaenoic acid (EPA, 20:5n-3) are generally low in the western population.¹ Therefore, increased intake of EPA and other n-3 polyunsaturated fatty acids (PUFA) is hypothesized to ameliorate a range of risk factors that contribute toward cardiometabolic diseases.² Notably, EPA has garnered attention as the recent REDUCE-IT trial showed EPA ethyl esters (Vascepa) substantially reduced the risk of cardiovascular disease in statin-treated patients with elevated triglycerides.³ As a consequence, the FDA approved EPA ethyl esters for cardiovascular disease risk reduction for select clinical populations. This overturned the dogma on n-3 PUFAs as having no efficacy for lowering the risk of cardiovascular diseases.⁴

The effects of n-3 PUFAs on insulin sensitivity and glucose tolerance remain strongly debated. Several randomized clinical trials have failed to establish the benefits of increased n-3 PUFA intake for treating subjects with insulin resistance, which may be due to a range of factors including poor controls, a focus on treatment rather than prevention, and often a neglect for a diversified human genetic makeup.^{2,5,6} Furthermore, a unifying mechanism by which n-3 PUFAs such as EPA prevent insulin resistance remains unclear. Many studies have relied on heterogeneous mixtures of n-3 PUFAs despite evidence that EPA and its long chain counterpart docosahexaenoic acid (DHA) are not structurally or functionally identical.⁷⁻⁹ To further complicate matters, many preclinical studies rely on levels of n-3 PUFAs that are not easily achievable in humans.² Finally, very little is known about the therapeutic potential of EPA-derived metabolites, which represent the next generation of n-3 PUFA research. Thus, the overarching goal of this study was to address these limitations.

We first studied if pure EPA ethyl esters, modeling human pharmacological intake, prevent obesity-induced metabolic

impairments using C57BL/6J mice. Supporting translational analyses on the association between fasting glucose levels and dietary intake of PUFAs were conducted using data from the National Health and Nutrition Examination Survey (NHANES).¹⁰ We then conducted mass spectrometry-based metabolomic and lipidomic analyses to identify targets of EPA ethyl esters, which led to the study of 18-hydroxyeicosapentaenoic acid (18-HEPE) and its downstream metabolite, resolvin E1 (RvE1). RvE1 belongs to a family of PUFA-derived endogenous metabolites known as specialized pro-resolving mediators (SPMs) that are potent immunoresolvants.¹¹⁻¹⁶ We specifically investigated if exogenous treatment of 18-HEPE followed by studies with RvE1 could reverse hyperinsulinemia and hyperglycemia through the G-protein coupled receptor ERV1/ChemR23. Given that RvE1 is an immunoresolvent, immune profiling experiments using flow cytometry addressed if RvE1 mitigated metabolic impairments in obesity via an improvement in adipose tissue inflammation. Finally, to translate the research, we determined if the metabolic effects of RvE1 were dependent on the host genome, which is critical to investigate as humans are genetically heterogeneous. To do so, we utilized diversity outbred (DO) mice, a unique mouse population that models human genetic diversity.¹⁷ In parallel, we conducted supporting SNP analyses by mining the Ensembl database to identify genetic variation of EPA and RvE1 metabolizing genes in humans.

2 | MATERIALS AND METHODS

2.1 | Animal models, diets, and 18-HEPE/RvE1 administration

All murine experiments adhered to IACUC guidelines established by The University of North Carolina at Chapel Hill and East Carolina University for euthanasia and humane treatment

in addition to the NIH Guide for the Care and Use of Laboratory Animals. Euthanasia relied on CO₂ inhalation followed by cervical dislocation. C57BL/6J male mice of 5-6 weeks of age were fed lean control (10% kcal from lard, Envigo TD.160407) or high-fat (HF) (60% kcal from lard, Envigo TD.06414, Indianapolis, IN) diet in the absence or presence of EPA (Cayman, ≥93%, Ann Arbor, MI) ethyl esters (Envigo TD.160232) for 15 weeks. EPA in the HF diet accounted for 2% of total energy. For select studies, C57BL/6J male mice were purchased obese from Jackson at 18 weeks of age. They were acclimatized by feeding lean (10% lard, D12450B) or HF (60% lard, D12492) diets (Research Diets, New Brunswick, NJ) for an additional 2-3 weeks prior to conducting experiments. DO male mice (Jackson, Bar Harbor, ME) from generation 33 were obtained at 4 weeks of age and acclimated for 2 weeks. The DO population is derived from 144 Collaborative Cross lines obtained from Oak Ridge National Laboratory at generations F4-F12 of inbreeding.¹⁷ For some experiments, mice were administered 300 ng of 18-HEPE or RvE1 purchased from Cayman Chemical per day for four consecutive days.¹⁸

The ERV1/ChemR23 mutant mice were generated by CRISPR/Cas9-mediated genome editing. Benchling software was used to identify Cas9 guide RNAs flanking the coding sequences of the *Cmklr1* (*ERV1/ChemR23*) gene. Three guide RNAs at each end of the target sequence were selected for activity testing. The 5' and the 3' guide RNAs were designed to target near the 3' end of ERV1/ChemR23 intron 2 and the 3' UTR region after the stop codon in ERV1/ChemR23 exon 3, respectively. Guide RNAs were cloned into a T7 promoter vector followed by in vitro transcription and spin column purification. A mouse embryonic fibroblast cell line was transfected with guide RNA and Cas9 protein to perform functional testing. The guide RNA target site was amplified from transfected cells and analyzed by T7 Endonuclease 1 assay. Guide RNAs selected for genome editing in embryos were 5sg81T (protospacer sequence 5'-GAGATCGTTCACAACCC-3') and 3sg81T (protospacer sequence 5'-gCGGCCAGGGACGCTA-3'). A donor oligonucleotide of sequence 5'-CATACGAATGCAAAATAAAGACAAGAAATGGCAAAGGGGAGATCGTTCACAATAATGGGAGACATGCCGGGAGCCTTTGGGAATGCTCCAATGCCACTGAATTTTG-3'.

was included to facilitate homologous recombination to produce a deletion event. However, the founder animal did not have the same deletion junction as the donor oligonucleotide, suggesting the oligonucleotide did not participate in the deletion allele resolution in that founder. C57BL/6J zygotes were electroporated with 1.2 μM Cas9 protein, 94.5 ng/mL each guide RNA and 400 ng/mL of donor oligonucleotide and implanted in recipient pseudopregnant females. Resulting pups were screened by PCR for the presence of a deletion allele. One male founder was identified with a precise deletion between the cut sites of the electroporated guide RNAs. The

founder was mated to wild-type (WT) C57BL/6J females to establish a colony with the deletion allele. ERV1/ChemR23 animals were detected by PCR with primers *Cmklr1*-5ScF1 (5'-GGAGCAGGAAACAGAATAGGAC-3'), *Cmklr1*-3ScF1 (5'-ATCACCTTCTTCCTCTGCTGG-3') and *Cmklr1*-3ScR1 (5'-GGTTTGACTGTCATGTTGCCATA-3'). The schematic illustrating the generation of the ERV1/ChemR23 mutant allele by CRISPR/Cas9-mediated genome editing is described below in the results. These mice and WT littermate controls were also fed diets from Envigo.

2.2 | Body mass and insulin/glucose measurements

Metabolic studies including echo-magnetic resonance imaging (MRI) experiments were conducted as previously described.¹⁹ Briefly, mice were fasted for 5 hours prior to the establishment of baseline glucose values with a glucometer. For the glucose tolerance test, 2.5 g of dextrose (Sigma-Aldrich, St. Louis, MO) per kg lean mass was administered intraperitoneally.

2.3 | Studies with diversity outbred mice

Since every DO mouse is genetically unique, each mouse served as its own control. Baseline fasting insulin/glucose measurements were recorded once each DO mouse achieved ~14 g of fat mass as measured by Echo-MRI. The mice were then allowed 1 week to recover and subsequently i.p. injected for four consecutive days with 300 ng RvE1 per day.¹⁸ Fasting glucose and fasting insulin were again measured after RvE1 administration.

2.4 | Untargeted mass spectrometry-based metabolomics

Adipose tissue and liver were homogenized using a bead homogenizer and prepared for metabolomics using previously described methods.¹⁹ Samples were analyzed using liquid chromatography/mass spectrometry (LC/MS) and raw data were extracted and processed using Agilent Technologies Mass Hunter Profinder Version B.08.00 (Profinder) software in combination with Agilent Technologies Mass Profiler Professional Version 14 (MPP) as previously described.²⁰⁻²² An in-house database containing METLIN, Lipid Maps, Kyoto Encyclopedia of Genes and Genomes (KEGG), and Human Metabolomics Database (HMDB) was used to annotate metabolites based on exact mass, isotope ratios, and isotopic distribution with a mass error cutoff of 10 ppm. This corresponds to annotation at Metabolomics Standards Initiative (MSI) level 3.²³

To visualize clustering between the dietary groups we ran a principal component analysis (PCA) using all metabolites. We then determined statistically significant metabolites between obese mice and obese mice supplemented with EPA. One of the samples from the HF diet (HF_105) was an outlier from all the other samples and was excluded from analyses. We then calculated fold changes (EPA/HF). Next, using the validated significant metabolites with Log₂ fold changes ± 1.5 we standardized the abundances of the metabolites by assigning a Z-score for each sample based on the distribution of the given metabolite. We utilized the Z-scores to generate heatmaps annotated with the classification of each metabolite.

2.5 | Targeted mass spectrometry-based metabololipidomics

Analyses of PUFA-derived metabolites of visceral white adipose tissue, liver, and heart was conducted as previously described.²⁴ Lipid mediators were extracted using Strata-X 33- μ m 30 mg/1 mL SPE columns (Phenomenex, Torrance, CA). Quantitation of lipid mediators was performed using two-dimensional reverse phase HPLC tandem mass spectrometry (liquid chromatography/tandem mass spectrometry). All standards and internal standards used for the LC/MS/MS analysis were purchased from Cayman Chemical (Ann Arbor, Michigan, USA). All solvents and extraction solvents were HPLC grade or better.

2.6 | Flow cytometry analyses of differing immune cell populations in adipose tissue

Epididymal visceral adipose tissue was mechanically chopped and then digested with collagenase Type 4, DNase 1, and 0.5% fatty acid free bovine serum albumin in phosphate buffered saline (PBS) for 50 minutes at 37°C in an incubator shaker (120 RPM). Next, 0.5M EDTA was added with RPMI media and the cells were passed through a 70- μ m cell strainer rinsed with 2% fetal bovine serum (FBS) in PBS. The cells were centrifuged at 1400 RPM for 5 minutes at 4°C, primary adipocytes were aspirated off from the top layer of the supernatant and the pellet containing the stromal vascular cells (SVC) was then incubated with red blood cell lysis buffer for 1 minute on ice. Two percent FBS-PBS was added to the SVCs and centrifuged at 1400 RPM for 5 minutes at 4°C and then passed through a 40- μ m cell strainer. SVCs were stained with the following fluorophore-tagged antibodies obtained from BioLegend (San Diego, CA): Zombie Aqua, CD45 (PerCP-Cy5.5), CD11b (FITC), CD19 (APC-Cy7), F4/80 (PE), and MHCII (BV421). The following SVC subsets were analyzed using

a BD LSRII flow cytometer: CD45⁺CD11b⁻CD19⁺ (B cells), CD45⁺CD11b⁺F4/80⁺MHCII⁺ (macrophages), CD45⁺CD11b⁺F4/80⁺MHCII⁻ (macrophages). All data were analyzed in FlowJo and gates were drawn from fluorescence minus one controls.

2.7 | Analyses of NHANES database

The 2013-2014 NHANES database was mined for daily average intake of PUFAs with respect to age, sex, and BMI. Nutrient intake for NHANES is measured via the 2013-2014 USDA's Food and Nutrient Database for Dietary Studies (FNDDS). NHANES utilizes the FNDDS to code individual food/beverages and portion sizes reported by participants and the FNDDS includes nutrient values for calculating nutrient intake from ingested foods. We used Rv3.4.4 with the RNHANES package to retrieve the NHANES database. Graphical packages ggpubr and ggplot2 were used to generate all graphs and statistical annotations. The "Dietary Interview - Total Nutrient Intakes" section of the NHANES database was used to retrieve PUFA intake measurements based on a 24-hour dietary recall questionnaire. OGTT 2-hour glucose measurements were retrieved from the "Current Health Status" section, where BMI was retrieved from "Body Measures." Tertiles of PUFA intake were calculated corresponding to the probability of intake at 33.3%, 67%, and 100% of the range. Normality and homogeneity of variance were tested with the Shapiro-Wilks test and Bartlett test, respectively. Since the dataset did not satisfy the assumptions of normality and heteroscedasticity, we utilized a Kruskal-Wallis test followed by a Wilcoxon pairwise test to measure significant differences between tertiles of PUFA intake.

2.8 | SNP analyses

We used the Biomart tool to mine the Ensembl Variation 98 Human Short Variants (GRCh38.p13) database for single nucleotide polymorphisms (SNPs) with minor allele frequencies at or above 5% that are contained within the 1000 genomes project or the NCBI dbSNP archive. We used the ggplot2 package in R v3.4.4 to plot all the minor allele frequencies by each allele for every gene and chromosome. White lines in the graph represent a break/gap in the minor allele frequency (MAF) distribution, for example, a gene may contain MAFs ranging from 0.05 to 1.5 then 2.5 to 4.5 with a "break" between 1.5 and 2.5 gap. The distance between SNPs of different genes on the chromosomes was determined using the base pair location at the last SNP of the first gene and the first SNP of the second gene. Distances below 500 kilobases were considered as having a higher likelihood for genetic linkage, as described by the HapMap project Haploview tool.

SNPs were mined in the following genes: PTGS2/COX2 (ENSG00000073756), CYP1A1 (ENSG00000140465), CYP1A2 (ENSG00000140505), CYP2E1 (ENSG00000130649), CYP2C8 (ENSG00000138115), CYP2C9 (ENSG00000138109), CYP2C18 (ENSG00000108242), CYP2C19 (ENSG00000165841), CYP2J2 (ENSG00000134716), CYP4F2 (ENSG00000186115), CYP4F3 (ENSG00000186529), CYP4F8 (ENSG00000186526), CYP4F12 (ENSG00000186204), CYP2S1 (ENSG00000167600), CMKLR1/ChemR23 (ENSG00000174600), LTB4R/BLT1 (ENSG00000123903), ALOX12/15 (ENSG00000108839 & ENSG00000161905), ALOX5 (ENSG0000012779), ALOX5AP/FLAP (ENSG00000132965) and LTA4H (ENSG00000111144).

2.9 | Statistics

Data were analyzed using Graph Pad Prism Version 7.0. Statistical significance relied on one-way or two-way ANOVAs followed by a post hoc Tukey HSD test if the data satisfied the assumptions of normality and homogeneity of variance tested by the Shapiro-Wilks test and Bartlett test, respectively. Data that failed the assumption of heteroscedasticity were analyzed using a Welch ANOVA followed by a pairwise Welch T test with a Bonferroni p-value adjustment. Datasets that did not display normal distributions were analyzed with a Wilcoxon pairwise test. Studies as a function of time that passed the assumptions of normality and heteroscedasticity were analyzed with a two-way ANOVA. For clarity, additional description of analyses are also included with each corresponding methods section above. For all analyses, $P < .05$ was considered statistically significant.

3 | RESULTS

3.1 | EPA limits hyperglycemia, hyperinsulinemia, and improves glucose tolerance of obese male C57BL/6J mice

We first determined if dietary administration of EPA could prevent obesity-induced metabolic impairments of obese male mice. The approach relied on pure ethyl esters of EPA and not mixtures of EPA with DHA that can confound the data. Mice consuming a HF diet in the absence or presence of EPA had similar increases in total mass and fat mass compared to lean controls (Figure 1A). Inclusion of EPA in the diet of obese mice prevented the development of obesity-driven glucose intolerance (Figure 1B), as quantified by the area under the curve (Figure 1C). Relative to the HF diet, EPA restored the impairment in fasting glucose (Figure 1D) and

improved fasting insulin levels (Figure 1E). The HOMA-IR score was also lowered with EPA in the diet, relative to the mice consuming the HF diet (Figure 1F).

3.2 | EPA is associated with improved glucose levels in obese humans in a sex-dependent manner

To translate the murine data, we analyzed the relation between EPA intake and blood glucose levels during an OGTT in obese humans using data from NHANES. Increased EPA intake was associated with lower glucose levels between the first tertile and the third tertile for obese males (Figure 2A) but not females (Figure 2B). Furthermore, we investigated if there was a relationship between DHA and glucose levels. In obese males (Figure 2C) and females (Figure 2D), there was no association between DHA and blood glucose levels.

The metabolism of EPA relies on some of the same immune responsive and metabolic enzymes used by n-6 PUFAs such as linoleic acid (LA).^{25,26} Thus, we further mined the NHANES data to determine if there was a relationship between the ratio of LA and EPA on fasting glucose levels. Tertiles of the LA to EPA ratio are plotted for obese men (Figure 2E) and women (Figure 2F). The positive association between EPA and glucose levels was diminished and strikingly, at the highest ratio of LA to EPA in men (Figure 2E), but not women (Figure 2F), blood glucose levels were increased relative to the first two tertiles. We also analyzed the ratio of arachidonic acid (AA) to EPA given that AA is also a highly prevalent n-6 PUFA. Analyses of the tertiles of the AA to EPA ratio showed no association with blood glucose levels in men (Figure 2G) and women (Figure 2H).

3.3 | Mice consuming EPA have a distinct metabolome compared to obese mice in the absence of EPA

As the mechanism of action for EPA ethyl esters is likely to be pleiotropic, we conducted metabolic profiling of mice consuming the experimental diets. PCA plots revealed a clear distinction between the control, HF, and HF + EPA ethyl ester diets for visceral white adipose tissue (Figure 3A). EPA ethyl esters were predominately incorporated into triglycerides with some uptake into diglycerides and phosphatidylcholine (Figure 3B,C). In the liver, PCA plots also showed a clear distinction between the HF and HF + EPA ethyl ester diets (Figure 3D). EPA ethyl esters appeared to have a broad effect on the liver metabolome (Figure 3E,F). EPA acyl chains were likely distributed into triglycerides, phosphatidylcholine, phosphatidylethanolamine, and anandamide

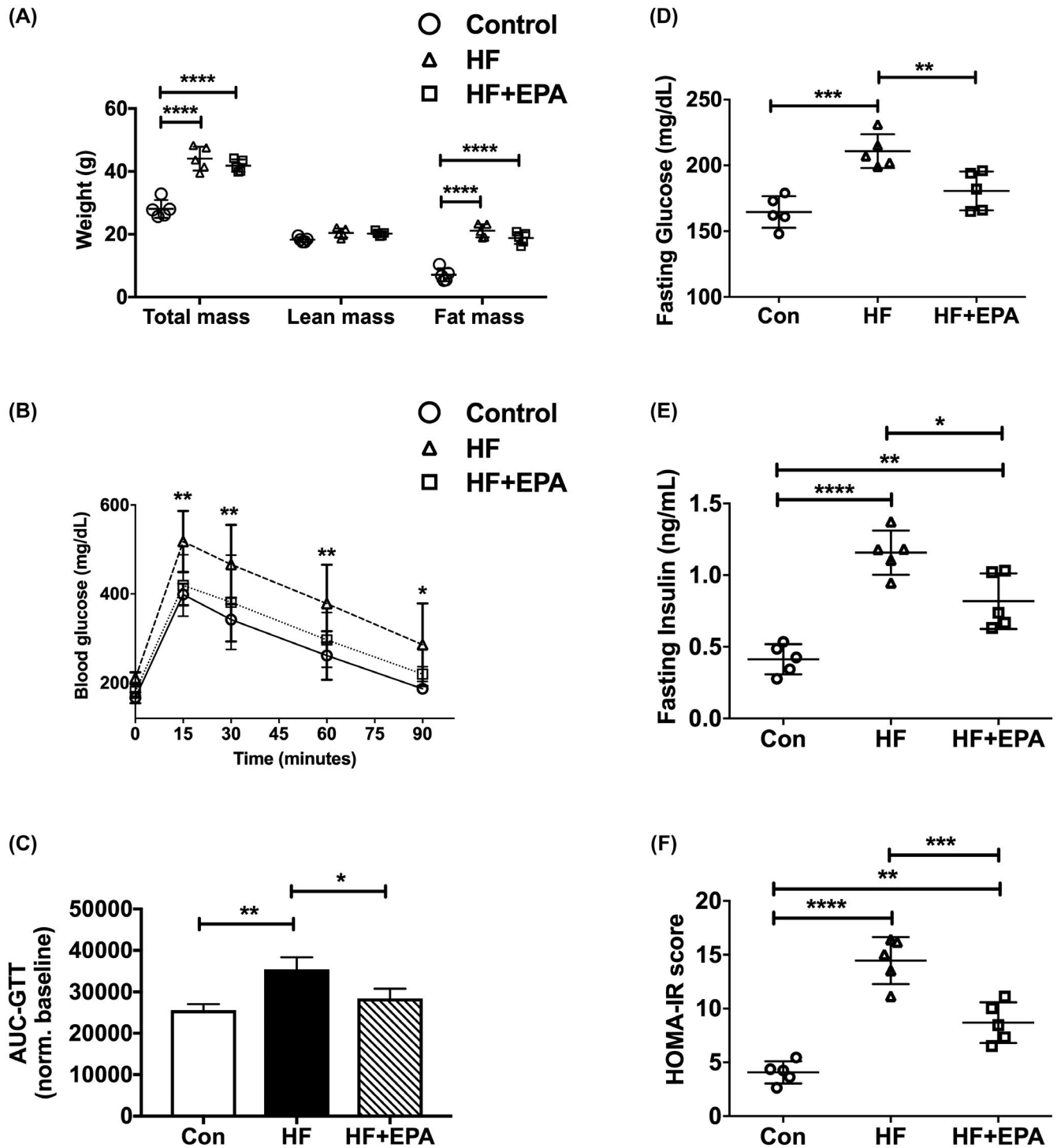


FIGURE 1 EPA ethyl esters prevent obesity-induced impairments in glucose tolerance, fasting glucose and fasting insulin levels of C57BL/6J mice. A, Body composition measured by Echo-MRI. B, Glucose tolerance test performed by intraperitoneal injection of glucose after a 5 h fast. C, Area under the curve (AUC), calculated by integration of the curves in B normalized to baseline values. D, Fasting glucose and (E) fasting insulin levels after a 5 h fast. F, HOMA-IR scores. For all measurements, male mice consumed a lean control (Con) diet (O), a high-fat (HF) diet (Δ), or a HF diet supplemented with EPA ethyl esters (\square). Measurements were conducted at week 13 of intervention. Values are means \pm SD. * $P < .05$, ** $P < .01$, *** $P < .001$, **** $P < .0001$ from one-way ANOVA followed by Tukey's multiple comparisons test except B, which was a two-way ANOVA followed by a post hoc test

(Figure 3F). Overall, these results showed that EPA ethyl esters incorporated into several lipid pools, which would then differentially influence metabolic pathways, particularly in

the adipose tissue and liver. The full metabolite names, P -values, fold changes, and quantitations are in Supporting Tables S1 and S2.

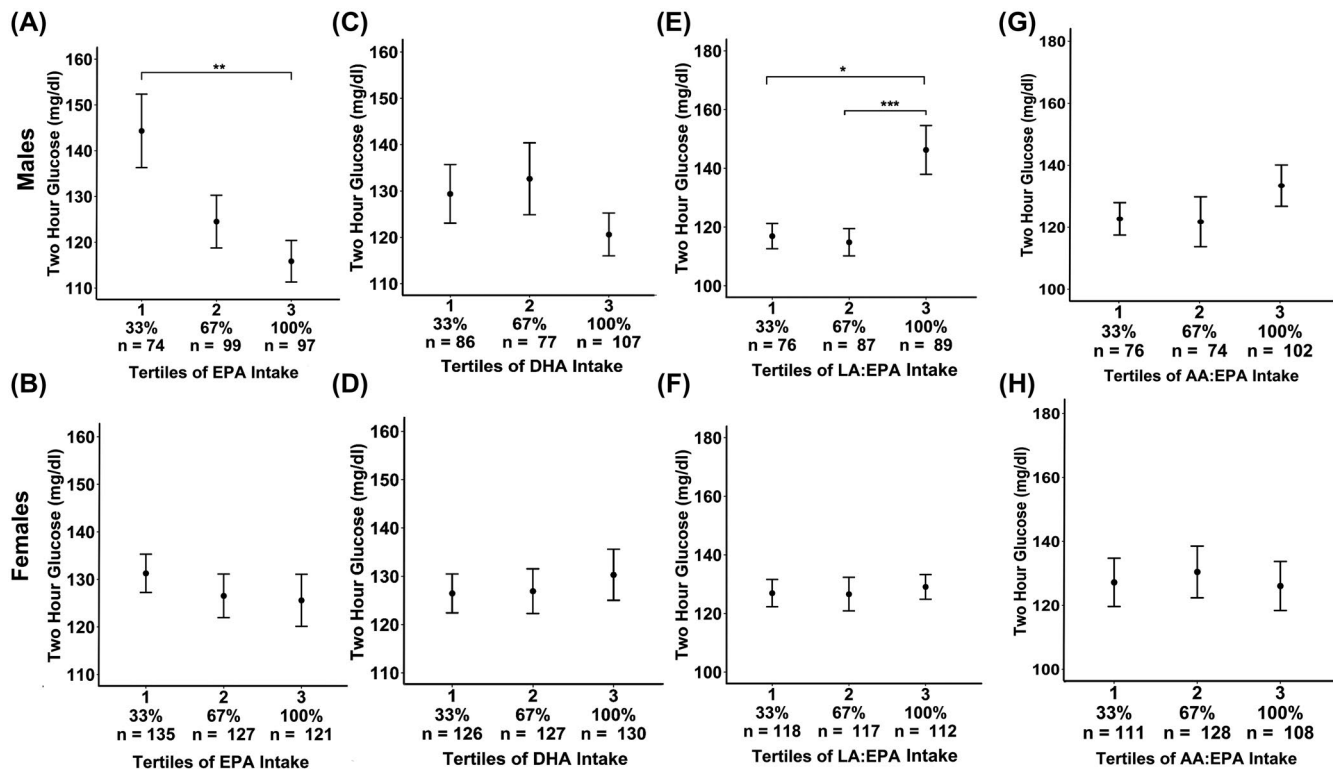


FIGURE 2 Glucose levels are inversely related to EPA intake in obese men but not women and are dependent on the ratio of LA to EPA. NHANES data on 2-hour glucose measurements (mg/dL) from an OGTT were stratified by tertiles of EPA intake in grams for obese (A) males and (B) females. DHA intake is also depicted for (C) males and (D) females. The range of EPA intake for males was 0.0-0.009 g for tertile 1, 0.01-0.068 g for tertile 2, 0.069 g, and above for tertile 3. For females, the intake is 0-0.009 for tertile 1, 0.01-1.51 g for tertile 2, 1.52 g, and above for tertile 3. The range of DHA intake for males is 0.01-0.05 g for tertile 1, 0.06-1.49 g for tertile 2, and 1.5 g and above for tertile 3. The range of DHA intake for females was 0.01-0.03 g for tertile 1, 0.04-2.35 g for tertile 2, and 2.36 g and above for tertile 3. Subjects were adults (18 years and older) and had a BMI of 30 and above. Tertiles of the ratio of LA to EPA are presented for obese (E) males and (F) females. Tertiles of the ratio of AA to EPA are presented for obese (G) males and (H) females. The tertiles correspond to 33%, 67%, and 100% of the range of LA to EPA intake for subjects older than 18 and a BMI of 30 and above. Values are means \pm SEM * P < .05, ** P < .01, *** P < .001 from Wilcoxon pairwise test. Number of subjects for each tertile is listed on the x-axis

3.4 | 12-HEPE and 18-HEPE levels are lowered with obesity and reversed with EPA

We next conducted targeted metabolomic analyses to further study the effects of EPA on the adipose tissue and liver lipidomes. The HF diet and HF diet + EPA modulated several n-3 and n-6 PUFA-derived metabolites in these tissues. The HF diet amplified several white adipose tissue n-6 PUFA-derived mediators relative to the lean control (Figure 4A). These included 11(12)-EET, 14(15)-EET, 15R-LXA₄, 6- α -PG, 8-iso-15R-PGF2 α , 8-iso-PGF2 α , carboxylic TXA₂, 8S-HETE, and 15S-HETE. Inclusion of EPA in the HF diet also amplified some but not all of these metabolites (Figure 4A). Markedly, the HF diet lowered the levels of the EPA-derived 18-HEPE, which was reversed with EPA in the diet. 18-HEPE levels were elevated by ~5.6 and ~32.6-fold relative to the lean and HF diets, respectively (Figure 4A). EPA also strongly upregulated

the concentration of 12-HEPE in white adipose tissue by ~58-fold.

In the liver, the n-6 PUFA-derived LXA₄ and PGE₂ were increased with the HF diet relative to the lean control (Figure 4B). Notably, 12-HEPE and 18-HEPE levels were undetectable with the HF diet compared to the control. The HF + EPA diet lowered PGE₂ and 9-HODE levels and increased LXB₄ levels relative to the HF diet. The HF + EPA diet also decreased the levels of 13-HODE compared to the lean and HF diets (Figure 4B). EPA dramatically increased the levels of 12-HEPE and 18-HEPE compared to the lean and HF diets (Figure 4B). EPA also elevated the levels of 14-HDHA and 17-HDHA relative to the HF diet.

We also analyzed the heart to determine if the effects of EPA were limited to white adipose tissue and liver. In the heart, EPA had some modest effects on the number of n-6 PUFA derived metabolites modified relative to the HF diet (Supporting Figure S1). Similar to white adipose tissue and

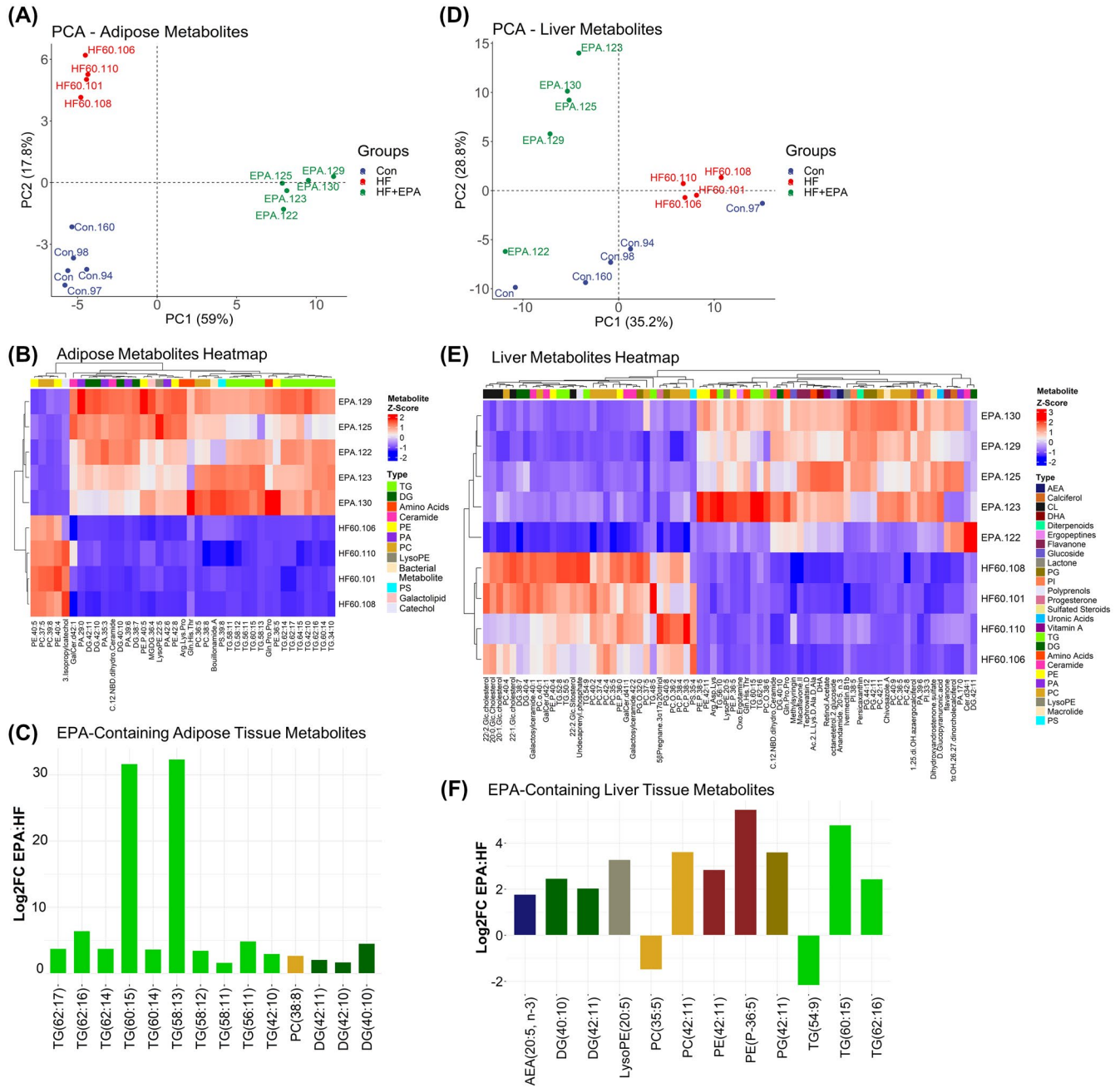


FIGURE 3 EPA ethyl esters have a distinct metabolomic profile in white adipose tissue and liver of obese C57BL/6J male mice. C57BL/6J male mice consumed a control (Con), high-fat (HF) and HF + EPA ethyl ester diet. A, PCA plot of validated adipose tissue metabolites between control, HF, and HF + EPA samples. B, Heatmap of Z-scores from significant adipose tissue metabolites with ± 1.5 fold-change. C, Log₂ fold change graph of EPA-containing (20:5) adipose metabolites. D, PCA plot of validated liver metabolites between control, HF, and HF + EPA samples. E, Heatmap of Z-scores from significant liver metabolites with ± 1.5 fold-change. F, Log₂ fold change graph of EPA-containing (20:5) adipose metabolites. Heatmap legends on the right hand side of (B) and (E) show each metabolite's classifications: triglyceride (TG), diacylglycerol (DG), phosphatidylethanolamine (PE), lysophosphatidylethanolamine (LysoPE), phosphatidic acid (PA), phosphatidylcholine (PC), phosphatidylserine (PS), phosphatidylglycerol (PG), phosphatidylinositol (PI), arachidonylethanolamine (AEA), cholesterol (CL), and docosahexaenoic acid (DHA). Full metabolite names are provided in the supplemental

liver, EPA increased the concentration of 12-HEPE and 18-HEPE by up to 11-27-fold relative to the lean and HF diets, respectively (Supporting Figure S1). Overall, the robust

amplification of 18-HEPE levels set the basis for subsequent experiments with 18-HEPE and RvE1, the downstream bioactive metabolite of 18-HEPE.

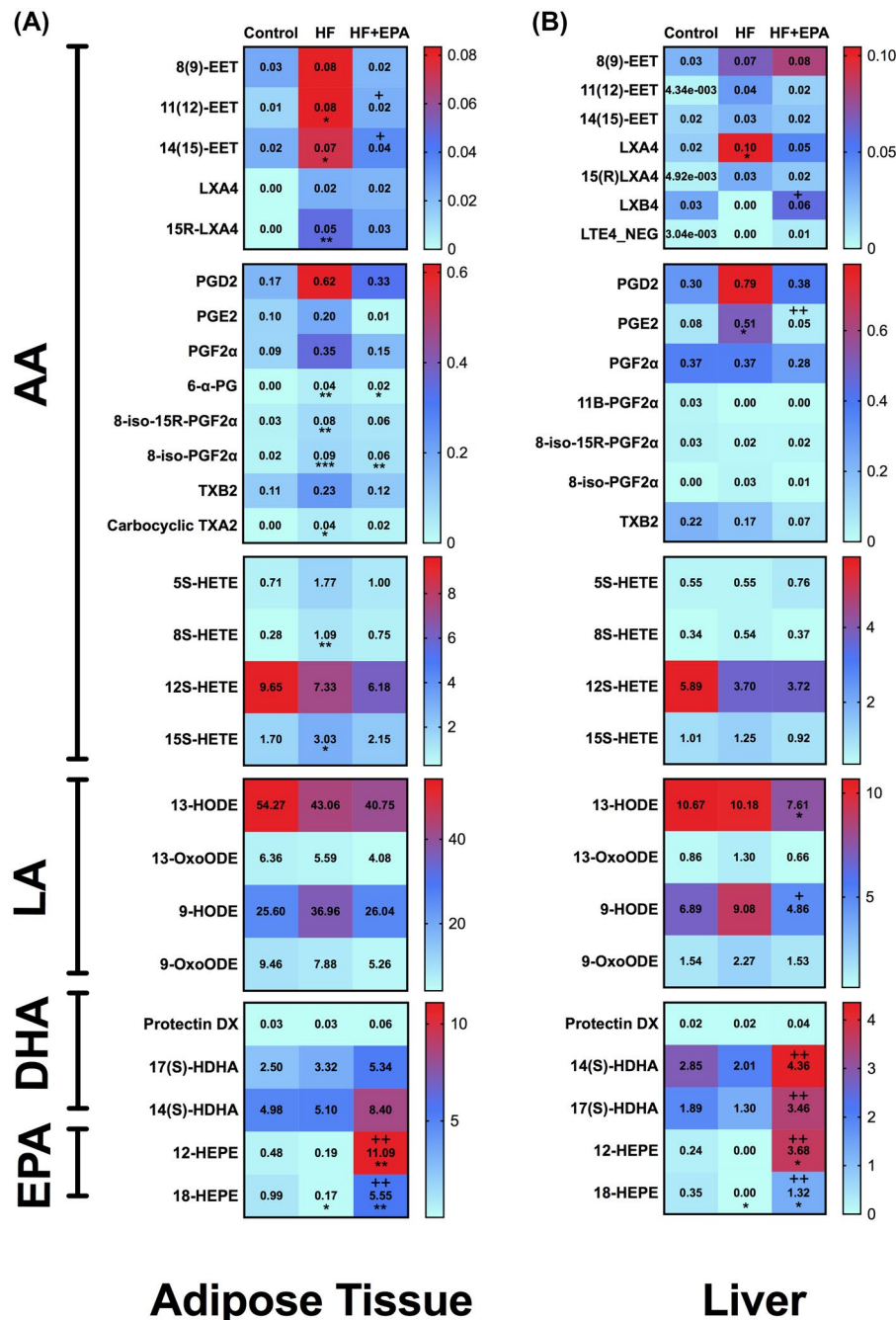


FIGURE 4 EPA ethyl esters reverse the effects of murine obesity on the concentration of 18-HEPE. Mass spectrometry-based metabolomic analyses of (A) visceral white adipose tissue and (B) liver. Metabolites from eicosapentaenoic acid (EPA), docosahexaenoic acid (DHA), linoleic acid (LA), and arachidonic acid (AA) are depicted in the heat map. Male C57BL/6J mice consumed experimental diets for 15 weeks. N = 4-5 mice per diet. Data are average. * $P < .05$, ** $P < .01$, *** $P < .001$ as compared to a control diet and + $P < .05$, ++ $P < .01$ as compared to the high-fat diet. Statistical analyses for these data are described in the methods section

3.5 | RvE1 but not 18-HEPE treatment improves hyperinsulinemia and controls hyperglycemia of inbred mice in a manner that is dependent on the receptor ERV1/ChemR23

We investigated the effects of 18-HEPE and RvE1 on fasting insulin and fasting glucose levels using C57BL/6J mice

(Figure 5A). For this specific study (Figure 5A-G), we used C57BL/6J mice that were obtained obese from Jackson Laboratories. 18-HEPE treatment of obese mice had no effect on body weight (Figure 5B) compared to the mice on a HF diet. 18-HEPE treatment also had no effect on fasting glucose (Figure 5C) and fasting insulin levels (Figure 5D) compared to mice on the HF diet. Experiments with RvE1 similarly

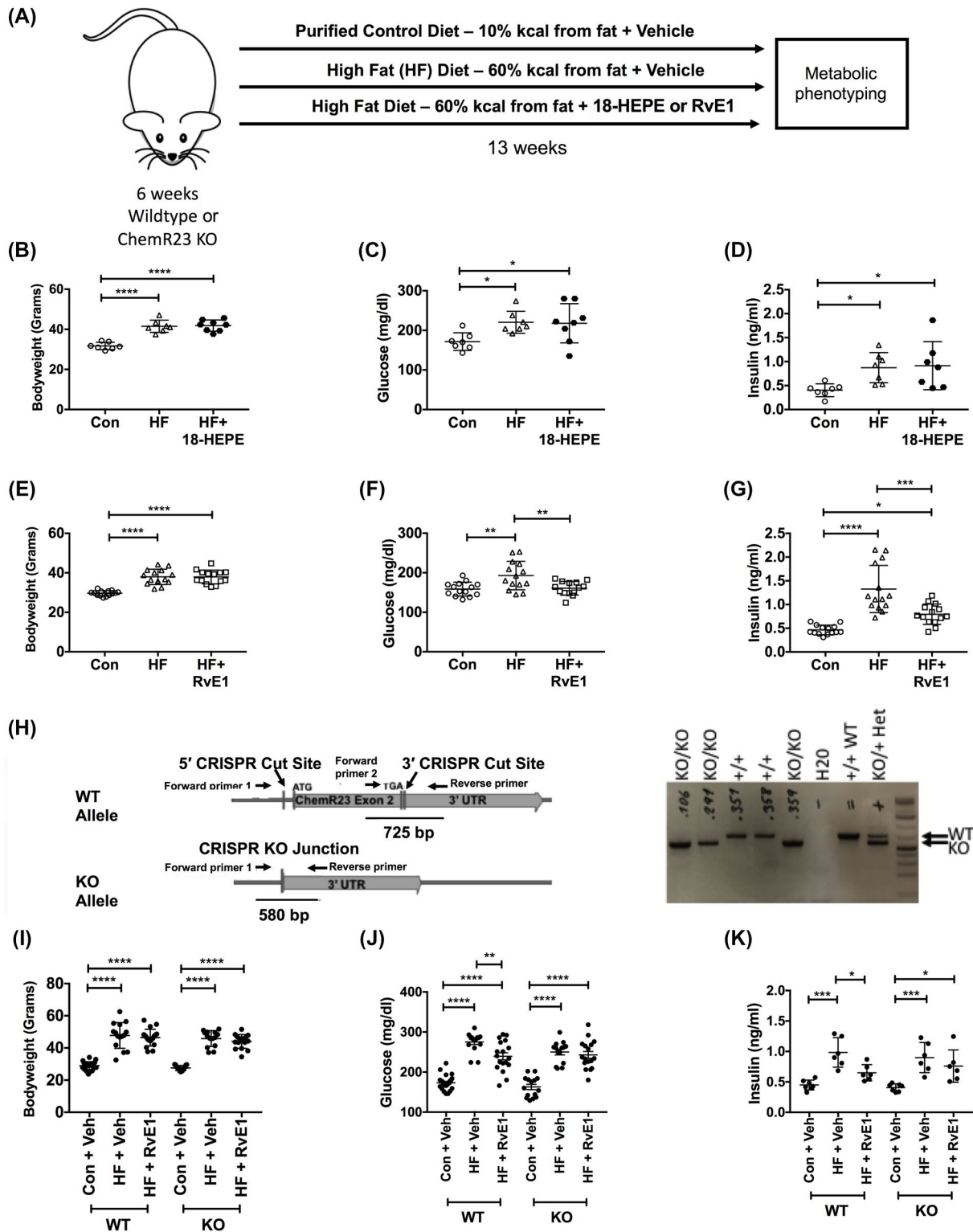


FIGURE 5 RvE1 but not 18-HEPE treatment improves obesity-driven impairments in fasting glucose and insulin of C57BL/6J mice mediated by the receptor ERV1/ChemR23. A, Study design for experiments using C57BL/6J mice or ERV1/ChemR23 knockout mice and their wild-type (WT) littermate controls administered 18-HEPE, RvE1 or vehicle control after being fed a high-fat diet or lean control diet. B, Body weight, (C) fasting glucose, and (D) fasting insulin levels of male C57BL/6J mice in the presence of 18-HEPE or vehicle control. E, Body weight, (F) fasting glucose, and (G) fasting insulin levels of C57BL/6J male mice in the presence of RvE1 or vehicle control. Experiments shown in B-G were with mice purchased obese from Jackson Laboratories. H, Illustration of ChemR23 deletion allele and genotyping. I, Body weight (J) fasting glucose, and (K) fasting insulin levels of male WT and ERV1/ChemR23 knockout (KO) mice consuming a lean control diet (Con) or high-fat (HF) diet in the presence of RvE1 or vehicle control. All measurements were made at 13-14 weeks of dietary intervention. N = 6-18 mice per diet. Values are means \pm SD. * $P < .05$, ** $P < .01$, *** $P < .001$, **** $P < .0001$ by one-way ANOVA followed by Tukey's multiple comparisons test

showed no effect on body weight (Figure 5E). However, RvE1 treatment improved fasting glucose (Figure 5F) and fasting insulin levels (Figure 5G) relative to obese mice.

We next tested the hypothesis that the effects of RvE1 was mediated by one of its two receptors known as ERV1/ChemR23. Therefore, we generated ERV1/ChemR23 knock-out (KO) mice and WT littermates to measure the effects of RvE1 on hyperinsulinemia and hyperglycemia induced by consumption of a HF diet. Figure 5H depicts the ERV1/ChemR23 deletion allele. Body composition did not differ between obese WT and ERV1/Chem23 KO mice administered vehicle control or RvE1 (Figure 5I). RvE1 treatment improved fasting glucose levels of WT but not ERV1/ChemR23 KO mice compared to obese mice (Figure 5J). We also tested fasting insulin levels in a subset of our WT and KO mice via an ELISA. Fasting insulin levels were improved in response to RvE1 in WT obese mice but not in ERV1/ChemR23 KO obese mice relative to obese mice that received the vehicle control (Figure 5K).

Mechanistically, immune cells such as B lymphocytes and macrophages in white adipose tissue have a central role in maintaining metabolic homeostasis. Furthermore, previous work shows that resolvin D1 improves glycemic control by targeting the number of M1- and M2-like macrophages in white adipose tissue.¹² Thus, we investigated if RvE1 was preventing the enrichment of key immune cells in visceral white adipose tissue. The flow cytometry gating strategy is depicted in Figure 6A and fluorescence minus one controls are shown in Supporting Figure S2. For this select study, we only compared mice consuming a HF diet in the absence or presence of RvE1 as significant pooling of lean mice was required. Strikingly, the analyses revealed RvE1 had no effect on the percentage of CD45⁺CD11b⁻CD19⁺ B cells (Figure 6B), CD45⁺CD11b⁺F4/80⁺MHCII⁺ macrophages (Figure 6C), or CD45⁺CD11b⁺F4/80⁺MHCII⁻ macrophages (Figure 6D). Similarly, there was no effect of RvE1 on the number of CD45⁺CD11b⁻CD19⁺ B cells (Figure 6E), CD45⁺CD11b⁺F4/80⁺MHCII⁺ macrophages (Figure 6F), or CD45⁺CD11b⁺F4/80⁺MHCII⁻ macrophages (Figure 6G). We also probed if RvE1 had any impact on select inflammatory and metabolic transcripts. qRT-PCR analysis revealed no effect of RvE1 on the expression of *adiponectin*, *Tnfa*, *IL10*, and *GLUT-4* (data not shown).

3.6 | Host genetics define the treatment response to RvE1

Humans are metabolically heterogeneous with a diversified genetic makeup. Therefore, in order to translate the findings with inbred C57BL/6J mice, we determined whether host genetic differences lead to variations in the fasting insulin and fasting glucose response to RvE1. For these studies, we used

the translational DO mouse model that mimics human genetic diversity and variability.¹⁷ Similar to the human population, administration of a HF diet led to large variations in body weight gain of DO mice. Thus, we optimized an experimental design (Figure 7A) to selectively measure the effects of RvE1 on fasting insulin and fasting glucose. Mice that achieved ~14 g of fat mass (measured via Echo-MRI) over the course of the dietary intervention with a HF diet were used for these studies. The rationale for selecting ~14 g of fat mass was based on the studies with obese C57BL/6J mice (Figures 1 and 5) that were in this range of fat mass. Body weight gain of the DO mice is depicted in Supporting Figure S3. Relative to baseline, RvE1 improved fasting glucose (Figure 7B) and fasting insulin (Figure 7C) levels in only half of the obese DO mice. In contrast, using the same experimental design with C57BL/6J mice, fasting glucose (Figure 7D), and fasting insulin (Figure 7E) were more uniformly improved in response to RvE1 treatment.

The results with the DO mice led us to further investigate if there is strong genetic variation in RvE1- and EPA-metabolizing genes in humans. We mined the Ensembl database containing the dbSNP archive and 1000 genomes data (Supporting Table S3). We extracted all the CYP450 enzymes that have the capacity to metabolize EPA, further downstream enzymes leading to the production of E-series resolvins (COX2, ALOX5, FLAP, ALOX12/15, and LTA4H), and the two RvE1 receptors, ChemR23, and BLT1 (Figure 7F).²⁷⁻²⁹ The CYP450 genes contained many SNPs in close proximity (<500 kilobases) on the same chromosome, indicating a higher probability for genetic linkage, these include: CYP2C18 and CYP2C19 (~27 Kb apart), CYP2C19 and CYP2C9 (~84 Kb), CYP2C9 and CYP2C8 (~47 Kb), CYP1A1 and CYP1A2 (~24 Kb), CYP4F8 and CYP4F3 (~10 Kb), CYP4F3 & CYP4F12 (~10 Kb), and CYP4F12 and CYP4F2 (~181 Kb) (Figure 7G). We also found a large range of minor allele frequencies where SNPs for each gene are contained in chromosomes 1, 10, 12-15, 17, and 19 (Figure 7G,H). Genes with lower ranges of MAF ranging from 0.05 (5%) to 0.38 (38%) include BLT1, COX2, CYP2J2, CYP1A1, and CYP1A2. Surprisingly, all other genes contained many high MAFs with numerous SNPs in the 0.4 (40%)-0.5 (50%) range (Figure 7G,H). Taken together, these results showed high population variance in EPA—and RvE1—metabolizing genes.

4 | DISCUSSION

There is growing evidence from humans and rodents that obesity impairs the biosynthesis of SPMs and their precursors, which are predominately generated from dietary n-3 PUFAs including EPA.^{13,19,30,31} The loss of SPMs contributes toward a range of cardiometabolic complications including chronic

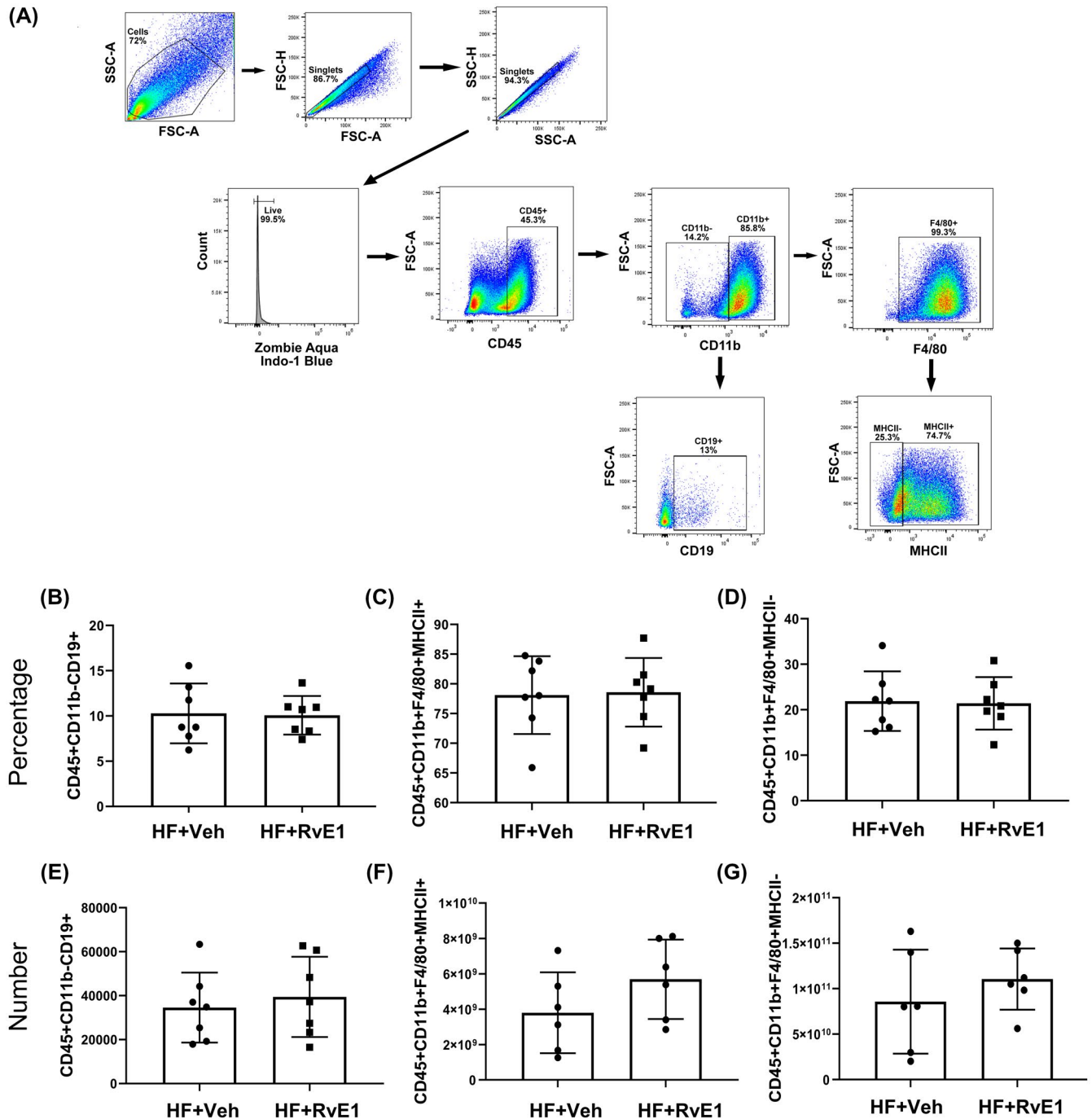


FIGURE 6 The metabolic improvement with RvE1 is not driven by a reduction in the enrichment of select inflammatory immune cells in white adipose tissue. A, Flow cytometry gating strategy for B lymphocytes and macrophage populations in the white adipose tissue of obese C57BL/6J male mice purchased from Jackson Laboratories. All measurements were made at 13-14 weeks of dietary intervention. The percentage of (B) CD45⁺CD11b⁻CD19⁺ B cells (C) CD45⁺CD11b⁺F4/80⁺MHCII⁺ macrophages and (D) CD45⁺CD11b⁺F4/80⁺MHCII⁻ macrophages. The number of (E) CD45⁺CD11b⁻CD19⁺ B cells, (F) CD45⁺CD11b⁺F4/80⁺MHCII⁺ macrophages and (G) CD45⁺CD11b⁺F4/80⁺MHCII⁻ macrophages. N = 6-7 mice per diet. Values are means \pm SD

inflammation, hepatic steatosis, insulin resistance, susceptibility to infection, and delayed wound healing.^{12,14,24,31-34} Therefore, there is an unmet need to understand how specific dietary n-3 PUFAs through the biosynthesis of their downstream metabolites regulate outcomes in cardiometabolic and inflammatory diseases.

Our study suggests that administration of EPA ethyl esters can prevent hyperinsulinemia and control hyperglycemia, in part, through the actions of RvE1 in a host genetic dependent manner. Given that EPA has a wide range of targets, its effects are likely pleiotropic and could involve other mechanisms such as remodeling of the microbiome, regulating brown

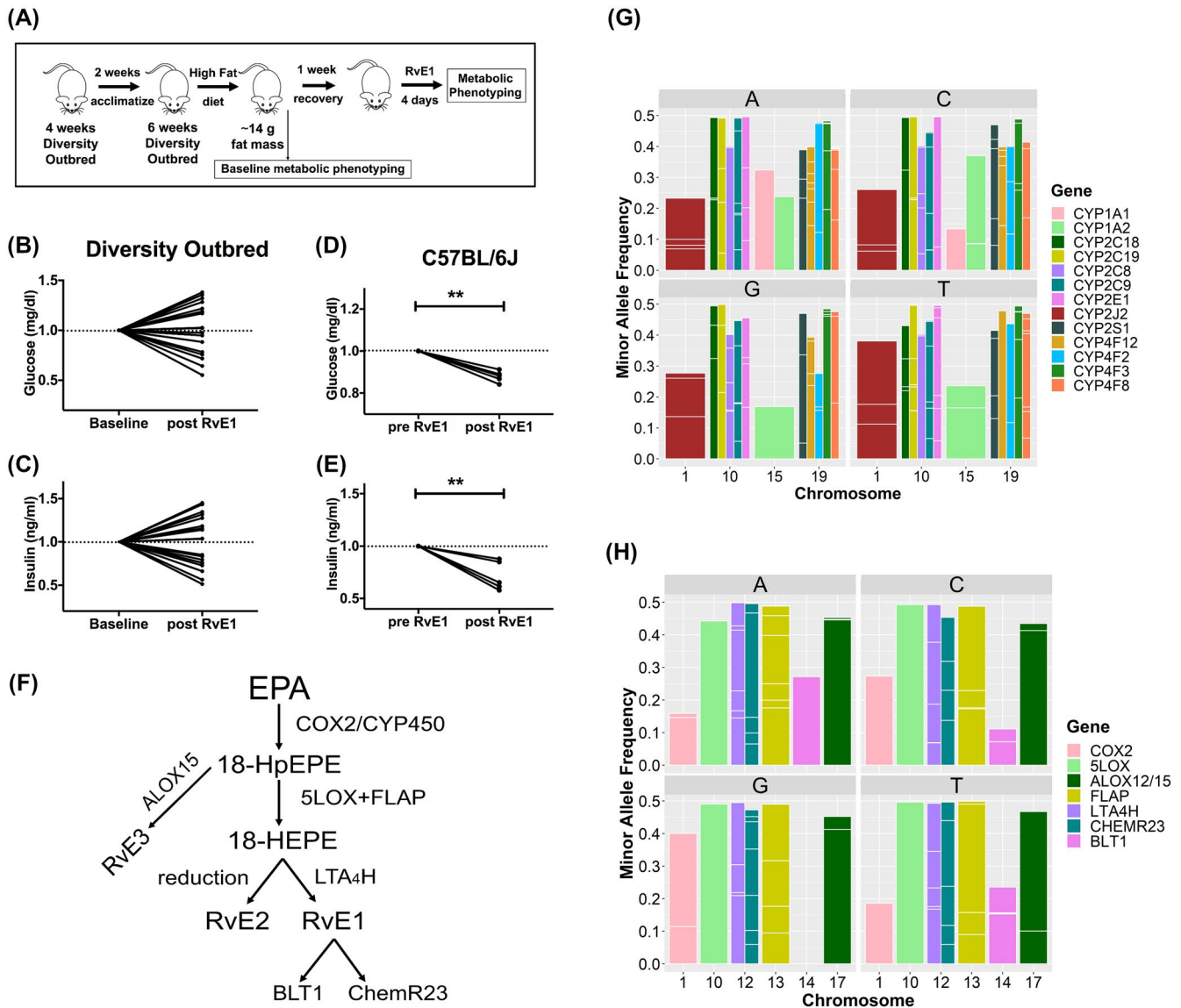


FIGURE 7 Host genetics have a critical role in the metabolic response to RvE1. A, Schematic representation of study design with diversity outbred mice. Fasting glucose and insulin measurements were obtained prior to (baseline) and after 4 days of RvE1 administration. B, Fasting glucose and (C) fasting insulin levels after a 5 h fast. Corresponding studies with C57BL/6J mice using the same experimental design of intervention are depicted for (D) fasting glucose and (E) fasting insulin. All data are plotted as the fold change in glucose and insulin relative to baseline. $N = 19$ DO mice and $N = 6$ C57BL/6J mice. $**P < .01$ by a paired two-tailed t test. F, Pathway of EPA metabolism leading to downstream metabolites including the biosynthesis of RvE1 and its receptors. Data were mined from the 1000 genomes and dbSNP human variants databases. Analyses show SNPs in the EPA and RvE1 metabolizing genes stratified by each minor allele (A,C,G,T). SNPs are depicted for (G) CYPs and (H) COX, 5-LOX, ALOX 12/15, FLAP, LTA₄H, ChemR23, and BLT1. The SNPs in each gene are plotted by minor allele frequencies and the chromosome that contains the SNP. The major genes that metabolize EPA and/or RvE1 are depicted by differing colors

adipose tissue metabolism, targeting transcription factors, or biophysical changes of immune cell plasma membranes.³⁵⁻³⁸ A notable outcome were the data from the NHANES analyses, which underscore the need for preventative precision nutrition studies with EPA. Longitudinal studies with EPA that are focused on prevention, prior to the onset of insulin resistance, are limited. One pilot study demonstrated that administration of n-3 PUFAs to healthy human volunteers prevented insulin resistance induced with a glucocorticoid.³⁹ The NHANES analyses revealed those subjects with lowest

consumption of EPA, but not DHA, had the highest glucose levels in a sex-specific manner. The positive effects of EPA were mitigated when the intake of LA was high, which is common in the western diet. While these data are associative, they point to the importance of discriminating EPA from DHA and accounting for LA levels in clinical studies and trials. LA biosynthesis and metabolism requires some of the same enzymes used for EPA synthesis and metabolism, including the endogenous biosynthesis of downstream metabolites such as RvE1.^{25,26} Indeed, a recent study showed that LA inhibited

the biosynthesis of select SPM precursors.⁴⁰ Moreover, LA's consumption in the western diet is 14–18 times the amount required to prevent LA deficiency^{2,41} and LA's effects on insulin sensitivity are debated.⁴² LA is an essential signaling PUFA for human and animal health, but its overconsumption may contribute toward chronic inflammation and metabolic impairments.

The data with EPA ethyl esters challenge previous findings. Earlier studies reported a reduction in fat mass with EPA-containing oils, which we did not observe.^{35,43} The differences in results using EPA ethyl esters compared to previous findings on body weight maybe due to the concentration/purity of EPA, duration, and use of EPA/DHA mixtures. EPA driving an upregulation in the concentration of RvE1's precursor is highly consistent with a recent clinical trial to show that consumption of an n-3 PUFA supplement promoted a strong upregulation of SPMs within 24 hours.⁴⁴

A major advancement is that our data show RvE1 could improve hyperinsulinemia and hyperglycemia via ERV1/ChemR23. RvE1 treatment is likely exerting its effects through multiple mechanisms. There is evidence that RvE1 blocks signaling through BLT1, the receptor for the arachidonic acid-derived LTB4.¹⁵ The pro-inflammatory mediator LTB4 serves as a chemokine for select immune cell populations that exacerbate glucose intolerance, particularly in white adipose tissue.⁴⁵ We did not find evidence that RvE1 is targeting the enrichment of immune cell populations in the adipose tissue as reported for resolvin D1.¹² Therefore, RvE1 must be targeting immune cells in other metabolic tissues as discussed below. The data are consistent with a study to show that protectin DX could improve insulin resistance independent of an effect on adipose tissue inflammation.¹⁶ We did find that RvE1's parent compound EPA lowered some n-6 PUFA-derived mediators, which could also influence the long-term inflammatory milieu.

Resolvin E1 activation of ERV1/ChemR23 may be further inhibiting signaling through chemerin, an adipokine that binds ERV1/ChemR23.⁴⁶ At the organ and cellular level, RvE1 can improve inflammation through the targeting of intestinal alkaline phosphatase and specific cell types including neutrophils as well as through the production of further downstream metabolites such as 18-oxo-RvE1.^{31,34,47,48} The effects of RvE1 are likely to occur simultaneously with other EPA-derived metabolites. Notably, we observed EPA strongly upregulated the concentration of 12-HEPE, which was recently identified to improve glucose metabolism.⁴⁹ In addition, EPA may also be exerting its effects through RvE2 and RvE3, which is an area of future investigation.

There is some ambiguity among studies regarding the effects of RvE1 on hyperglycemia. Overexpression of ERV1/ChemR23 in myeloid cells improved hyperglycemia and hepatic steatosis of male mice.⁵⁰ However, RvE1 administration to WT mice at a dose of 2ng/g body weight twice weekly for

4 weeks did not improve hyperglycemia.⁵⁰ Our studies relied on a higher dose of RvE1 (300ng/mouse) for four consecutive days, which may explain the positive effects. Overall, our data on RvE1 were in agreement with the literature to show that select DHA-derived SPMs such as protectin DX and resolvin D1 improve insulin resistance and enhance glucose tolerance.^{12,16,32,51–53}

Given the robust effect of RvE1 on hyperinsulinemia, we speculate that RvE1 could be targeting pancreatic islet size and insulin secretion from beta cells. To support this possibility, the Van Dyke group showed that myeloid overexpression of ERV1/ChemR23 led to an increase in the proportion of islet insulin-producing cells and islet size relative to mice on a HF diet.⁵⁰ The underlying mechanism may be driven by improvements in pancreatic macrophage-driven inflammation, which was recently identified to be a major driver of impairments in insulin secretion.⁵⁴ In support of this view, there is evidence from an in vitro study that RvE1 treatment lowers the expression of pro-inflammatory markers in human islets. Furthermore, ERV1/ChemR23 activation stimulates ERK phosphorylation and calcium influx in the pancreas.^{55,56} Therefore, our studies set the basis for studying distinct inflammatory populations in the pancreas such as intra-islet and peri-islet macrophages that control insulin secretion.⁵⁴ It is important to note that RvE1 may also be targeting other aspects of insulin and glucose metabolism as is relates to the liver and skeletal muscle.

A final advancement from this study is that DO mice, which model human genetic diversity, respond in a divergent manner upon RvE1 administration. The results open a new area of investigation by suggesting that RvE1 is unlikely to have a uniform positive effect in all obese humans. These results underscore the need for precision treatment in the human population. A future direction with the DO mice is to establish quantitative trait loci that control the metabolic response to RvE1 in obesity. This will set the basis for validating key genes using genetically modified mouse models and analyses of human SNPs. Overall, little is known about the role of host genetics on SPM biology. One study highlights the importance of genetic variation by demonstrating that obese subjects with a C allele in the rs1878022 polymorphism of ERV1/ChemR23 receptor confers protection from adipose tissue inflammation.⁵⁷

The study with DO mice directly informs emerging clinical trials with EPA-derived metabolites on the need to account for the host genome. To exemplify, a recent placebo controlled randomized trial with a 15-hydroxy EPA ethyl ester (Epeleuton) showed an improvement in glycemic control, HbA1c, and inflammation in adults with nonalcoholic fatty liver disease.⁵⁸ Therefore, future studies that account for host genetics may find more robust effects with the use of precision clinical trials. The results with the DO mice provide strong groundwork for studies that will establish candidate

genes regulating the metabolic response to RvE1. This will allow investigators to establish “responders” from “non-responders” to EPA-derived metabolites in humans.

Mining the 1000 genomes and dbSNP databases revealed a large range of minor allele frequencies in the EPA- and RvE1-metabolizing genes. Most of the genes analyzed reach minor allele frequencies close to 50%, indicating large population variance in the EPA-RvE1 pathway. Furthermore, close proximity of the CYP450 enzyme SNPs suggest potential genetic linkage in many of the CYP450 variants that can potentially influence metabolism of EPA and its downstream metabolites. There are numerous polymorphisms in the CYP enzymes related to various metabolic diseases.⁵⁹ For instance, CYP2C8, CYP2C9, and CYP2C19 contain SNPs that have been associated with increased susceptibility to type 2 diabetes in the Indian, Japanese, and Saudi populations.⁶⁰⁻⁶³ The etiology and risk of developing type 2 diabetes has also been associated with the COX2 rs5275 variant in type 2 diabetic patients.⁶⁴ Furthermore, SNPs in FLAP or LTA₄-H are correlated with a two-fold risk for myocardial infarction and stroke.^{65,66} SNPs in 5-LOX (ALOX5) have also been associated with modest increases in body mass index.⁶⁷ These studies highlight the importance of understanding genetic variants in the RvE1 response as numerous polymorphisms in the EPA metabolic pathway are common with potential clinical implications.

In summary, the results provide strong evidence that the EPA-RvE1 axis has a critical role in controlling insulin and glucose homeostasis, which may be a preventative target for cardiometabolic diseases. The results across model systems highlight the need for future prevention and treatment studies that account for the role of host genetics in the metabolism of RvE1 and other EPA-derived metabolites.

ACKNOWLEDGMENTS

We thank Dr Dale Cowley from the UNC Animal Models Core for his assistance in generating the ERV1/ChemR23 KO mice.

CONFLICT OF INTEREST

RPB has received industrial grants, including those matched by the Canadian government, and/or travel support related to work on brain fatty acid uptake from Arctic Nutrition, Bunge Ltd., DSM, Fonterra, Mead Johnson, Nestec Inc, and Pharmavite. Moreover, RPB is on the executive of the International Society for the Study of Fatty Acids and Lipids and held a meeting on behalf of Fatty Acids and Cell Signaling, both of which rely on corporate sponsorship. RPB has given expert testimony in relation to supplements and the brain. SRS has previously received industry grants including research related to n-3 fatty acids from GSK and Organic Technologies.

AUTHOR CONTRIBUTIONS

A. Pal designed/performed research, analyzed data, wrote the paper; A.E. Al-Shaer designed/performed research, analyzed data, and wrote parts of the paper; W. Guesdon designed/performed research, analyzed data; M.J. Torres performed research, analyzed data; M. Armstrong performed research, analyzed data; K. Quinn performed research, analyzed data; T. Davis performed research; N. Reisdorph designed/performed research; P.D. Neuffer contributed analytical tools; E.E. Spangenburg contributed analytical tools; I. Carroll contributed analytical tools; R.P. Bazinet edited the paper; G.V. Halade edited the paper; J. Clària. edited the paper; and S.R. Shaikh designed research, analyzed data, contributed analytical tools, and wrote the paper.

REFERENCES

1. Stark KD, Van Elswyk ME, Higgins MR, Weatherford CA, Salem N. Global survey of the omega-3 fatty acids, docosahexaenoic acid and eicosapentaenoic acid in the blood stream of healthy adults. *Prog Lipid Res.* 2016;63:132-152.
2. Lalia AZ, Lanza IR. Insulin-sensitizing effects of omega-3 fatty acids: lost in translation? *Nutrients.* 2016;8(6):329.
3. Bhatt DL, Steg PG, Miller M, et al. Cardiovascular Risk Reduction with Icosapent Ethyl for Hypertriglyceridemia. *N Engl J Med.* 2019;380:11-22.
4. Aung T, Halsey J, Kromhout D, et al. Associations of omega-3 fatty acid supplement use with cardiovascular disease risks: meta-analysis of 10 trials involving 77 917 individuals. *JAMA Cardiol.* 2018;3:225-234.
5. Brown TJ, Brainard J, Song F, Wang X, Abdelhamid A, Hooper L. Omega-3, omega-6, and total dietary polyunsaturated fat for prevention and treatment of type 2 diabetes mellitus: systematic review and meta-analysis of randomised controlled trials. *BMJ.* 2019;366:l4697.
6. Coelho OGL, da Silva BP, Rocha DMUP, Lopes LL, de Alfenas RCG. Polyunsaturated fatty acids and type 2 diabetes: impact on the glycemic control mechanism. *Crit Rev Food Sci Nutr.* 2017;57:3614-3619.
7. Leng X, Kinnun JJ, Cavazos AT, et al. All n-3 PUFA are not the same: MD simulations reveal differences in membrane organization for EPA, DHA and DPA. *Biochim Biophys Acta Biomembr.* 2018;1860:1125-1134.
8. Klingel SL, Metherel AH, Irfan M, et al. EPA and DHA have divergent effects on serum triglycerides and lipogenesis, but similar effects on lipoprotein lipase activity: a randomized controlled trial. *Am J Clin Nutr.* 2019;110:1502-1509.
9. Mason RP, Libby P, Bhatt DL. Emerging mechanisms of cardiovascular protection for the omega-3 fatty acid eicosapentaenoic acid. *Arterioscler Thromb Vasc Biol.* 2020;40:1135-1147.
10. Ahluwalia N, Dwyer J, Terry A, Moshfegh A, Johnson C. Update on NHANES dietary data: focus on collection, release, analytical considerations, and uses to inform public policy. *Adv Nutr.* 2016;7:121-134.
11. Arita M, Bianchini F, Aliberti J, et al. Stereochemical assignment, antiinflammatory properties, and receptor for the omega-3 lipid mediator resolvin E1. *J Exp Med.* 2005;201:713-722.

12. Hellmann J, Tang Y, Kosuri M, Bhatnagar A, Spite M. Resolvin D1 decreases adipose tissue macrophage accumulation and improves insulin sensitivity in obese-diabetic mice. *FASEB J*. 2011;25:2399-2407.
13. Neuhofer A, Zeyda M, Mascher D, et al. Impaired local production of proresolving lipid mediators in obesity and 17-HDHA as a potential treatment for obesity-associated inflammation. *Diabetes*. 2013;62:1945-1956.
14. González-Pérez A, Horrillo R, Ferré N, et al. Obesity-induced insulin resistance and hepatic steatosis are alleviated by omega-3 fatty acids: a role for resolvins and protectins. *FASEB J*. 2009;23:1946-1957.
15. Sima C, Paster B, Van Dyke TE. Function of pro-resolving lipid mediator resolvin E1 in type 2 diabetes. *Crit Rev Immunol*. 2018;38:343-365.
16. White PJ, St-Pierre P, Charbonneau A, et al. Protectin DX alleviates insulin resistance by activating a myokine-liver glucoregulatory axis. *Nat. Med.* 2014;20:664-669.
17. Churchill GA, Gatti DM, Munger SC, Svenson KL. The diversity of outbred mouse population. *Mamm. Genome*. 2012;23:713-718.
18. Hamlett ED, Hjorth E, Ledreux A, Gilmore A, Schultzberg M, Granholm AC. RvE1 treatment prevents memory loss and neuroinflammation in the Ts65Dn mouse model of Down syndrome. *Glia*. 2020;68:1347-1360.
19. Crouch MJ, Kosaraju R, Guesdon W, et al. Frontline science: a reduction in DHA-derived mediators in male obesity contributes toward defects in select B cell subsets and circulating antibody. *J Leukoc Biol*. 2019;106:241-257.
20. Yang Y, Cruickshank C, Armstrong M, Mahaffey S, Reisdorph R, Reisdorph N. New sample preparation approach for mass spectrometry-based profiling of plasma results in improved coverage of metabolome. *J Chromatogr A*. 2013;1300:217-226.
21. Cruickshank-Quinn CI, Mahaffey S, Justice MJ, et al. Transient and persistent metabolomic changes in plasma following chronic cigarette smoke exposure in a mouse model. *PLoS One*. 2014;9:e101855.
22. Quinn KD, Schedel M, Nkrumah-Elie Y, et al. Dysregulation of metabolic pathways in a mouse model of allergic asthma. *Allergy*. 2017;72:1327-1337.
23. Sumner LW, Amberg A, Barrett D, et al. Proposed minimum reporting standards for chemical analysis Chemical Analysis Working Group (CAWG) Metabolomics Standards Initiative (MSI). *Metabolomics*. 2007;3:211-221.
24. Kosaraju R, Guesdon W, Crouch MJ, et al. B cell activity is impaired in human and mouse obesity and is responsive to an essential fatty acid upon murine influenza infection. *J Immunol*. 2017;198:4738-4752.
25. Choque B, Catheline D, Rioux V, Legrand P. Linoleic acid: between doubts and certainties. *Biochimie*. 2014;96:14-21.
26. Innes JK, Calder PC. Omega-6 fatty acids and inflammation. *Prostaglandins Leukot Essent Fatty Acids*. 2018;132:41-48.
27. Westphal C, Konkel A, Schunck W-H. CYP-eicosanoids—a new link between omega-3 fatty acids and cardiac disease? *Prostaglandins Other Lipid Mediat*. 2011;96:99-108.
28. Fer M, Dréano Y, Lucas D, et al. Metabolism of eicosapentaenoic and docosahexaenoic acids by recombinant human cytochromes P450. *Arch Biochem Biophys*. 2008;471:116-125.
29. Frömel T, Kohlstedt K, Popp R, et al. Cytochrome P4502S1: a novel monocyte/macrophage fatty acid epoxygenase in human atherosclerotic plaques. *Basic Res Cardiol*. 2013;108:319.
30. López-Vicario C, Titos E, Walker ME, et al. Leukocytes from obese individuals exhibit an impaired SPM signature. *FASEB J*. 2019;33:7072-7083.
31. Clària J, Dalli J, Yacoubian S, Gao F, Serhan CN. Resolvin D1 and resolvin D2 govern local inflammatory tone in obese fat. *J Immunol*. 2012;189:2597-2605.
32. Titos E, Rius B, López-Vicario C, et al. Signaling and immunore-solving actions of resolvin D1 in inflamed human visceral adipose tissue. *J Immunol*. 2016;197:3360-3370.
33. Tang Y, Zhang MJ, Hellmann J, Kosuri M, Bhatnagar A, Spite M. Proresolution therapy for the treatment of delayed healing of diabetic wounds. *Diabetes*. 2013;62:618-627.
34. Freire MO, Dalli J, Serhan CN, Van Dyke TE. Neutrophil resolvin E1 receptor expression and function in type 2 diabetes. *J Immunol*. 2017;198:718-728.
35. Pahlavani M, Razafimanjato F, Ramalingam L, et al. Eicosapentaenoic acid regulates brown adipose tissue metabolism in high-fat-fed mice and in clonal brown adipocytes. *J Nutr Biochem*. 2017;39:101-109.
36. Caesar R, Tremaroli V, Kovatcheva-Datchary P, Cani PD, Bäckhed F. Crosstalk between gut microbiota and dietary lipids aggravates WAT Inflammation through TLR signaling. *Cell Metab*. 2015;22:658-668.
37. Magee P, Pearson S, Whittingham-Dowd J, Allen J. PPAR γ as a molecular target of EPA anti-inflammatory activity during TNF- α -impaired skeletal muscle cell differentiation. *J Nutr Biochem*. 2012;23:1440-1448.
38. Teague H, Harris M, Fenton J, Lallemand P, Shewchuk BM, Shaikh SR. Eicosapentaenoic and docosahexaenoic acid ethyl esters differentially enhance B-cell activity in murine obesity. *J Lipid Res*. 2014;55:1420-1433.
39. Delarue J, Li C-H, Cohen R, Corporeau C, Simon B. Interaction of fish oil and a glucocorticoid on metabolic responses to an oral glucose load in healthy human subjects. *Br J Nutr*. 2006;95:267-272.
40. Marchix J, Catheline D, Duby C, et al. Interactive effects of maternal and weaning high linoleic acid intake on hepatic lipid metabolism, oxylipins profile and hepatic steatosis in offspring. *J Nutr Biochem*. 2020;75:108241.
41. Naughton SS, Mathai ML, Hryciw DH, McAinch AJ. Linoleic acid and the pathogenesis of obesity. *Prostaglandins Other Lipid Mediat*. 2016;125:90-99.
42. Jandacek RJ. Linoleic acid: a nutritional quandary. *Healthcare*. 2017;5(2):25.
43. Pinel A, Pitois E, Rigaudiere J-P, et al. EPA prevents fat mass expansion and metabolic disturbances in mice fed with a Western diet. *J Lipid Res*. 2016;57:1382-1397.
44. Souza PR, Marques RM, Gomez EA, et al. Enriched marine oil supplements increase peripheral blood specialized pro-resolving mediators concentrations and reprogram host immune responses: a randomized double-blind placebo-controlled study. *Circ Res*. 2020;126:75-90.
45. Li P, Oh DY, Bandyopadhyay G, et al. LTB4 promotes insulin resistance in obese mice by acting on macrophages, hepatocytes and myocytes. *Nat Med*. 2015;21:239-247.
46. Mariani F, Roncucci L. Chemerin/chemR23 axis in inflammation onset and resolution. *Inflamm Res*. 2015;64:85-95.
47. Campbell EL, MacManus CF, Kominsky DJ, et al. Resolvin E1-induced intestinal alkaline phosphatase promotes resolution of inflammation through LPS detoxification. *Proc Natl Acad Sci U S A*. 2010;107:14298-14303.

48. Herrera BS, Hasturk H, Kantarci A, et al. Impact of resolvin E1 on murine neutrophil phagocytosis in type 2 diabetes. *Infect Immun.* 2015;83:792-801.
49. Leiria LO, Wang C-H, Lynes MD, et al. 12-Lipoxygenase regulates cold adaptation and glucose metabolism by producing the omega-3 lipid 12-HEPE from brown fat. *Cell Metab.* 2019;30:768-783.e7.
50. Sima C, Montero E, Nguyen D, et al. ERV1 overexpression in myeloid cells protects against high fat diet induced obesity and glucose intolerance. *Sci Rep.* 2017;7:12848.
51. Jung TW, Ahn SH, Shin JW, et al. Protectin DX ameliorates palmitate-induced hepatic insulin resistance through AMPK/SIRT1-mediated modulation of fetuin-A and SeP expression. *Clin Exp Pharmacol Physiol.* 2019;46:898-909.
52. White PJ, Arita M, Taguchi R, Kang JX, Marette A. Transgenic restoration of long-chain n-3 fatty acids in insulin target tissues improves resolution capacity and alleviates obesity-linked inflammation and insulin resistance in high-fat-fed mice. *Diabetes.* 2010;59:3066-3073.
53. Martínez-Fernández L, González-Muniesa P, Laiglesia LM, et al. Maresin 1 improves insulin sensitivity and attenuates adipose tissue inflammation in ob/ob and diet-induced obese mice. *FASEB J.* 2017;31:2135-2145.
54. Ying W, Lee YS, Dong Y, et al. Expansion of islet-resident macrophages leads to inflammation affecting β cell proliferation and function in obesity. *Cell Metab.* 2019;29:457-474.e5.
55. Wittamer V, Franssen J-D, Vulcano M, et al. Specific recruitment of antigen-presenting cells by chemerin, a novel processed ligand from human inflammatory fluids. *J Exp Med.* 2003;198:977-985.
56. Goralski KB, McCarthy TC, Hanniman EA, et al. Chemerin, a novel adipokine that regulates adipogenesis and adipocyte metabolism. *J Biol Chem.* 2007;282:28175-28188.
57. López-Vicario C, Rius B, Alcaraz-Quiles J, et al. Association of a variant in the gene encoding for ERV1/ChemR23 with reduced inflammation in visceral adipose tissue from morbidly obese individuals. *Sci Rep.* 2017;7:15724.
58. Hamza M, Weissbach M, Coughlan D, Climax J, Bhatt DL. Abstract 13305: epeleuton, a novel synthetic second-generation N-3 fatty acid, decreased triglycerides, improved glycemic control and decreased markers of inflammation in a phase 2 exploratory study. *Circulation.* 2019;140:A13305.
59. Elfaki I, Mir R, Almutairi FM, Duhier FMA. Cytochrome P450: polymorphisms and roles in cancer, diabetes and atherosclerosis. *Asian Pac J Cancer Prev.* 2018;19:2057-2070.
60. Elfaki I, Almutairi FM, Mir R, Khan R, Abu-duhler F. Cytochrome p450 cyp1b1*2 gene and its association with t2d in tabuk population, northwestern region of saudi arabia. *Asian J Pharm Clin Res.* 2018;11:55.
61. Mahdi F, Raza ST, Rizvi S, Abbas S, Karoli R. Distribution of genetic polymorphisms in drug metabolizing gene cytochrome P450 (CYP2C8*3 and CYP2C9*2) in a north indian type 2 diabetes population. *Explor Res Hypothesis Med.* 2016;1(3):42.
62. Hoyo-Vadillo C, Garcia-Mena J, Valladares A, et al. Association of CYP2C19 genotype with type 2 diabetes. *Health.* 2010;2:1184-1190.
63. Yamada Y, Matsuo H, Watanabe S, et al. Association of a polymorphism of CYP3A4 with type 2 diabetes mellitus. *Int J Mol Med.* 2007;20:703-707.
64. Ozbayer C, Kebapci MN, Degirmenci I, Yagci E, Gunes HV, Kurt H. Genetic variant in the 3'-untranslated region of the COX2 gene is associated with type 2 diabetes: a hospital-based case-control study. *Prostaglandins Leukot Essent Fatty Acids.* 2018;137:39-42.
65. Helgadottir A, Manolescu A, Thorleifsson G, et al. The gene encoding 5-lipoxygenase activating protein confers risk of myocardial infarction and stroke. *Nat Genet.* 2004;36:233-239.
66. Crosslin DR, Shah SH, Nelson SC, et al. Genetic effects in the leukotriene biosynthesis pathway and association with atherosclerosis. *Hum Genet.* 2009;125:217-229.
67. Šerý O, Hlinecká L, Povová J, et al. Arachidonate 5-lipoxygenase (ALOX5) gene polymorphism is associated with Alzheimer's disease and body mass index. *J Neurol Sci.* 2016;362:27-32.

SUPPORTING INFORMATION

Additional Supporting Information may be found online in the Supporting Information section.

How to cite this article: Pal A, Al-Shaer AE, Guesdon W, et al. Resolvin E1 derived from eicosapentaenoic acid prevents hyperinsulinemia and hyperglycemia in a host genetic manner. *The FASEB Journal.* 2020;00:1–17. <https://doi.org/10.1096/fj.202000830R>